

# Elucidating the Body Surface P-wave using a Detailed Computer Model of Atrial Activation

Michael A Colman<sup>1</sup>, Daniele Giacomelli<sup>2</sup>, Phillip Langley<sup>2</sup>, Henggui Zhang<sup>1</sup>

<sup>1</sup>University of Manchester, Manchester, UK

<sup>2</sup>Newcastle University, Newcastle, UK

## Abstract

*Features of the ECG P-wave remain largely unexplained. P-wave notching is thought to relate to distinct events of right and left atrial activations. Wandering pacemaker is known to give rise to distinct P wave morphologies. In this study, we develop a 3D computational model of the human atria that is incorporated into a 3D human torso model which can simulate realistic P-waves across the torso. The atrial model considered detailed anatomical structure and electrophysiological heterogeneity. The torso model is used to produce ECG P-waves corresponding to those of the standard 12 lead ECG as well as a more detailed 64 lead electrode vest. The model is validated both in terms of the atrial activation sequence and the P-waves produced. The 12 lead ECG is then used to detect the presence of acetylcholine and isoprenaline on the atria. The 64 lead vest simulation is used to confirm that the presence of distinct P-wave modes in a clinical ECG is likely due to the presence of a leading pacemaker site shift, which may be caused by acetylcholine.*

## 1. Introduction

Features of the ECG P-wave remain largely unexplained. P-wave notching is thought to relate to distinct events of right and left atrial activations. Wandering pacemaker is known to give rise to distinct P wave morphologies and may be related to autonomic regulation of the heart. Such behaviours have yet to be characterised in detail. The standard 12 lead ECG is presently the most common non invasive method of monitoring the electrical activity of the heart in a clinical environment. However, the level of detail provided by such systems is highly limited. More complex multi lead arrays may be used to provide higher level of detail and hence assist in the diagnosis of arrhythmias. We present a computational model of the human atria and torso which is used to simulate P-waves from the standard 12 lead

ECG as well as a more detailed 64 lead ECG vest. We then use the model to investigate the detection of acetylcholine and isoprenaline on the atria, as well as shifts in the leading pacemaker site.

## 2. Methods

The single cell myocyte model describing the action potential (AP) of the human atria is developed based on the Courtemanche-Ramirez-Nattel (1998) model [1]. Into this, the  $\text{Ca}^{2+}$  handling system of the Koivumaki *et al.* (2011) model [2] is incorporated, along with new formulations for the sarcolemmal currents  $I_{\text{to}}$ ,  $I_{\text{Kur}}$ ,  $I_{\text{f}}$  and  $I_{\text{CaT}}$ . From this base model, a large range of regional cell models is developed, including the crista terminalis (CT), pectinate muscles (PM), right atrial appendage (RAA), Bachmann's bundle (BB), atrial septum (AS), left atrium (LA), pulmonary veins (PV) and those of the spontaneously depolarising sino atrial (SA) and atrioventricular (AV) nodes. Detailed electrophysiological models for the effect of acetylcholine (ACh) and isoprenaline (ISO) were also developed and incorporated into all of the regional cell models.

The 3D human atrial model is based on that of the visible human female dataset. To this, detailed anatomical models of the human SA node and AV node are incorporated. The model is then further segmented to include distinct regions for the PV, AVR, RAA and SA node block zone (Figure 1.A.). The gradient model is applied to the SA-node to replicate the heterogeneous behaviour observed experimentally. The well known monodomain equation [3] describing the propagation of the AP within the tissue is solved by the use of a centred finite different method.

The atrial model is then placed inside a human torso model, the geometry of which is taken from Weixue and Ling (1996) [4]. The model includes considerations for the lungs and the blood masses of the atria and ventricles (Figure 1. B(i)). The forward problem, describing propagation of the electrical activity from the surface of the atria to the surface of the body is solved by the use of a boundary element method. Then, elements of the torso

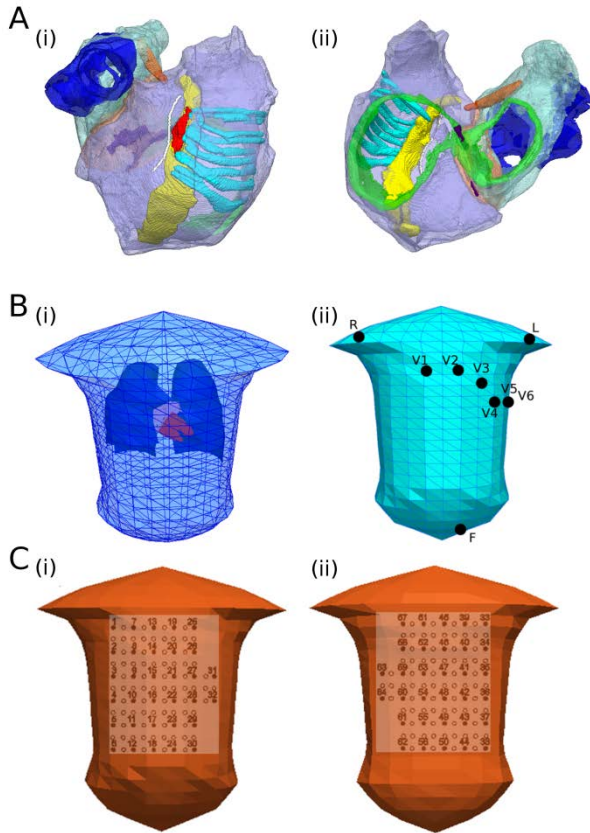


Figure 1. Human atrial and torso model. A. The human atrial model from (i) frontal view, (ii) view into the cavities. The regions are as follows: SA-node (red), PM (light blue), CT (yellow), RAA (transparent purple), BB (orange), block zone (white), AV-node (purple), AS (light orange), LA (transparent light blue), AVR (green) and PV (blue). B. Torso model. (i) Torso shown with the atria and lungs in place. (ii) Electrode placement for 12 lead ECG. C Electrode placement for 64 lead vest front (i), back (ii).

mesh were selected as those corresponding to the locations of the electrodes in the 12 lead ECG and 64 lead ECG vest (Figure 1.B(ii), C). These were used to produce P-waves corresponding to those produced clinically. The model is capable of spontaneously depolarising and hence does not need to be paced. To investigate the effects of ACh and ISO,  $0.5 \mu\text{Mol/L}$  of each is applied to the model and the resulting activation patterns and P-waves analysed. In the investigation of the effect of a leading pacemaker site shift on the P-waves produced by the 64-lead ECG vest, various locations along the CT and within the SAN were selected as stimulation points (Figure 2.). A stimulus of  $20 \text{ pA}$  was applied to each location for a duration of  $2 \text{ ms}$  at a basic cycle length of  $700 \text{ ms}$ . The resulting atrial activation from the 3<sup>rd</sup> stimulus is used to derive ECG P-waves.

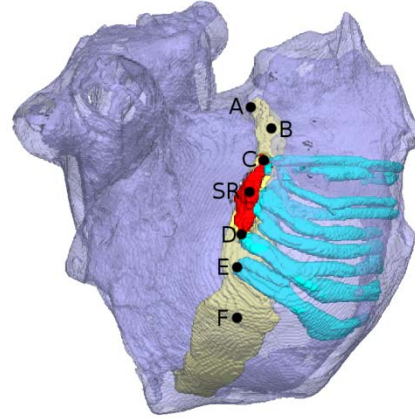


Figure 2. Locations used for the investigation of P-wave modes. SR corresponds to the location of the leading pacemaker site during sinus rhythm.

## 2. Results

The normal activation sequence of the atrial model closely corresponded quantitatively to that of Lemery *et al.* (2007) [5]. The activation sequence of the SA-node closely corresponded to that of Fedorov *et al.* (2010) [6].

To qualitatively validate the torso model, the simulated spatio-temporal distribution of the body surface potential (BSP) as a result of normal conduction patterns during sinus rhythm was compared to 64-lead BSP maps of P-waves from 10 healthy subjects. There was strong agreement in overall dipole direction and presence of P-wave notches. Quantitatively, the positive and negative peak of averaged P-waves occurs at  $\sim 60 \text{ ms}$  experimentally, compared to  $\sim 55 \text{ ms}$  in simulations. The body surface potential maps also closely corresponded to that of Mirvis *et al.* (1980) [7].

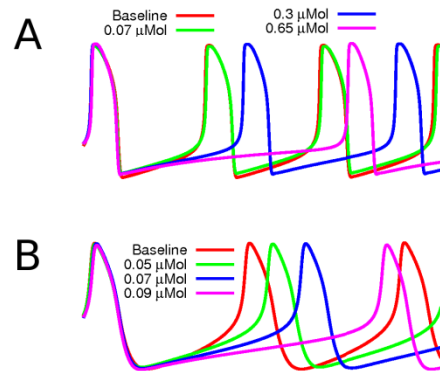


Figure 3. The effects of ACh on the SA-nodal peripheral (A) and central (B) cells, at varying concentrations

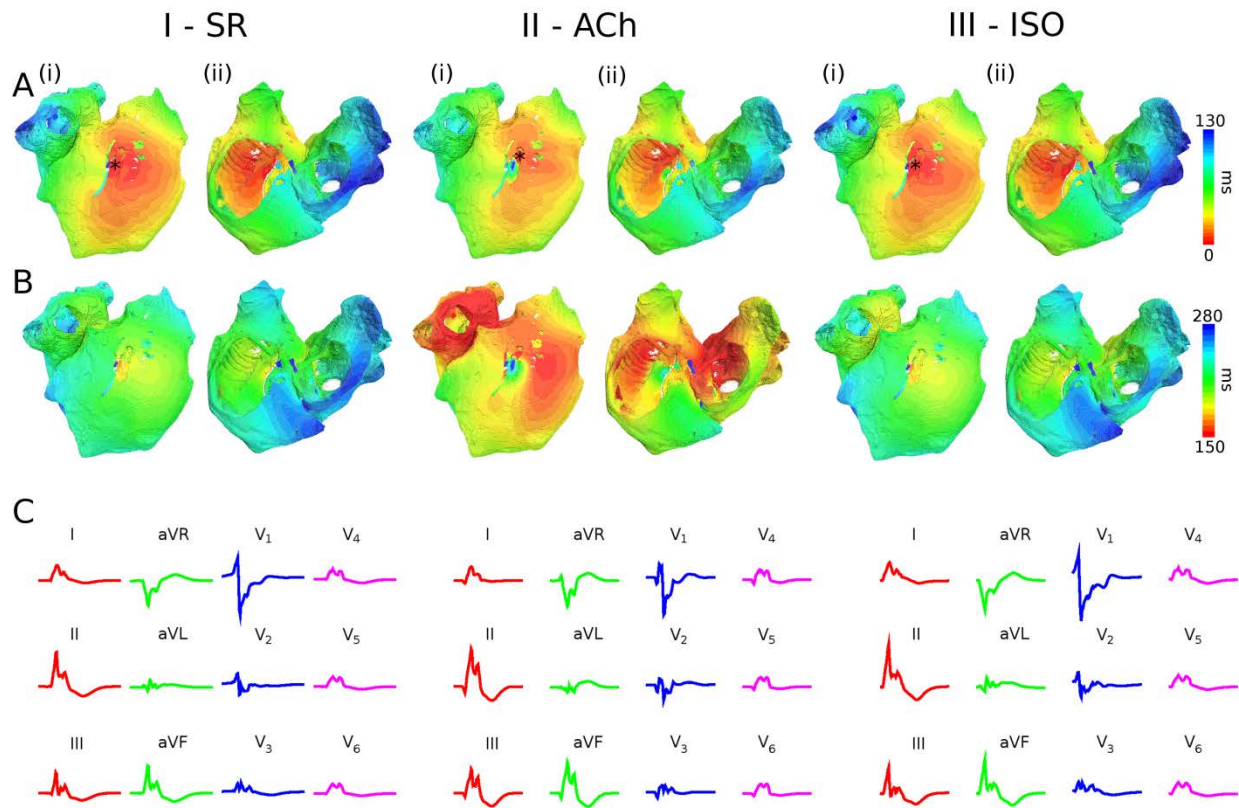


Figure 4. Effects of ACh and ISO on atrial activity and P-wave morphology. A. Atrial activation patterns, B. atrial repolarisation patterns and C. P-waves for sinus rhythm (I), ACh (II) and ISO (III). The asterisk indicates the location of the leading pacemaker site.

In single cell SA-nodal models, ACh affected the central and peripheral cells heterogeneously (Figure 3.) The pacing rate was reduced in both cases, but by a greater degree at lower concentrations in the central cell compared to the peripheral. ISO has the effect of heterogeneously increasing the pacing rate in both central and peripheral cells. Figure 4 shows the effects of ACh and ISO in 3D. ACh causes a shift in the leading pacemaker site which results in a distinct atrial activation pattern (Figure 4. (II) A), as has been observed in canine [8]. ISO causes no such shift (Figure 4. (III). A). Repolarisation occurs earlier with ACh than with ISO or during sinus rhythm (SR). The P-waves in leads II, III and aVF have a slightly greater magnitude with ACh, and exhibit more of a spiked peak with ISO. The P-T<sub>p</sub> interval is shortened with ACh, and both ISO and ACh cause an increased magnitude of the T<sub>p</sub> waves, due to a greater gradient of phase 3 repolarisation in the AP.

The results of the leading pacemaker site investigation are shown in Figure 4, compared to those observed clinically in one patient whom exhibited two distinct P-wave modes. The simulated P-waves shown correspond to those of sites C and D in Figure 2. Whereas the P-waves do not precisely match between experimental and simulated data, there is in general strong agreement. The differences between the two P-wave modes observed

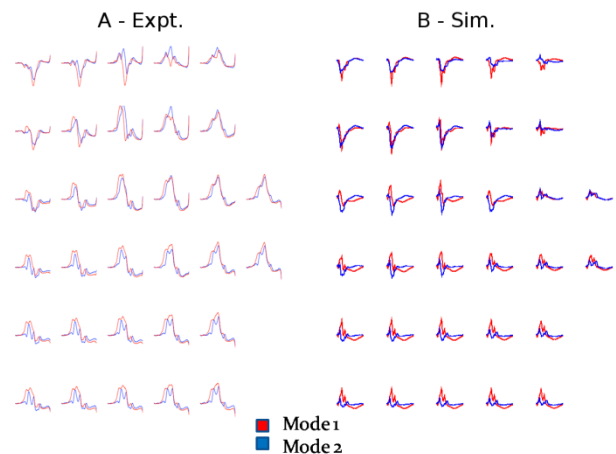


Figure 5. Two distinct P-wave modes observed clinically (A) and from the simulations (B). In B, mode 1 corresponds to site C and mode 2 to site D.

clinically is closely replicated by the differences between the simulated P-waves from these two sites. Hence, it is likely that the modes observed correspond to a shift in the leading pacemaker site. ACh is a likely cause of this, as the shift caused by ACh (Figure 6) is similar to that of the difference between sites C and D.

### 3. Conclusion

The 3D atrial and torso models developed have been validated experimentally and hence are suitable for the investigation of the monitoring of atrial activity using the 64 lead ECG vest. The results of the leading pacemaker site investigation suggest that such distinct P-wave modes may indeed be a result of a change in the leading pacemaker site within the SA-node. Such a leading pacemaker site shift can result from the effects of ACh on the SA-node. This in turn occurs due to its heterogeneous effects on the central and peripheral cells within the SA-node, highlighting the importance of consideration of such heterogeneities in accurate 3D modelling.

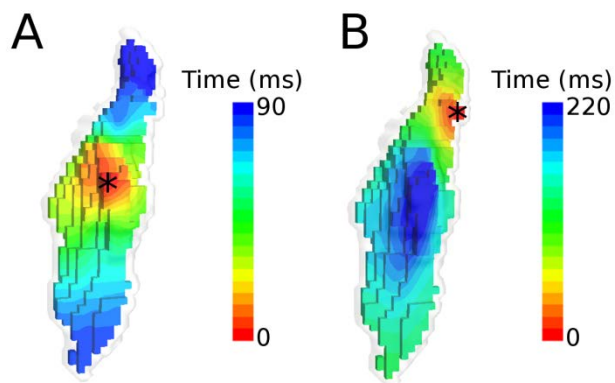


Figure 6. Leading pacemaker site shift due to ACh. A. SAN activation during SR and B. after the application of 0.5  $\mu\text{Mol}$  of ACh. The asterisk indicates the location of the leading pacemaker site.

### Acknowledgements

This work was funded by the EPSRC-DTA.

Address for correspondence.

Henggui Zhang  
Professor of Biological Physics  
School of Physics & Astronomy  
The University of Manchester  
Room 3.07 Schuster Building  
Brunswick Street  
Manchester, M13 9PL  
UK  
Tel: +44 (0)161 306 3966  
e-mail: [henggui.zhang@manchester.ac.uk](mailto:henggui.zhang@manchester.ac.uk)

### References

- [1] Courtemanche M, Ramirez RJ, Nattel S. Ionic mechanisms underlying human atrial action potential properties: insights from a mathematical model. *Am. J. Physiol.* 1998;275(1 Pt 2):H301–321
- [2] Koivumäki JT, Korhonen T, Tavi P. Impact of sarcoplasmic reticulum calcium release on calcium dynamics and action potential morphology in human atrial myocytes: a computational study. *PLoS Comput. Biol.* 2011;7(1):e1001067.
- [3] Aslanidi OV, Colman MA, Stott J, Dobrzynski H, Boyett MR, Holden AV, et al. 3D virtual human atria: a computational platform for studying clinical atrial fibrillation. *Prog. Biophys. Mol. Biol.* 2011;107(1):156–68.
- [4] Weixue L, Ling X. Computer simulation of epicardial potentials using a heart-torso model with realistic geometry. *IEEE Trans Biomed Eng.* 1996;43(2):211–7.
- [5] Lemery R, Birnie D, Tang ASL, Green M, Gollob M, Hendry M, et al. Normal atrial activation and voltage during sinus rhythm in the human heart: an endocardial and epicardial mapping study in patients with a history of atrial fibrillation. *J. Cardiovasc. Electrophysiol.* 2007;18(4):402–8.
- [6] Fedorov VV, Glukhov AV, Chang R, Kostecki G, Aferol H, Hucker WJ, et al. Optical mapping of the isolated coronary-perfused human sinus node. *J. Am. Coll. Cardiol.* 2010;56(17):1386–94.
- [7] Mirvis DM. Body surface distribution of electrical potential during atrial depolarization and repolarization. *Circulation.* 1980;62(1):167–73.
- [8] Fedorov VV, Chang R, Glukhov AV, Kostecki G, Janks D, Schuessler RB, et al. Complex interactions between the sinoatrial node and atrium during reentrant arrhythmias in the canine heart. *Circulation.* 2010;122(8):782–9.